Mifepristone Alters Amyloid Precursor Protein Processing to Preclude Amyloid Beta and Also Reduces Tau Pathology

David Baglietto-Vargas, Rodrigo Medeiros, Hilda Martinez-Coria, Frank M. LaFerla, and Kim N. Green

Background: Increased circulating glucocorticoids are features of both aging and Alzheimer's disease (AD), and increased glucocorticoids accelerate the accumulation of AD pathologies. Here, we analyzed the effects of the glucocorticoid receptor antagonist mifepristone (RU486) in the 3xTg-AD mouse model at an age where hippocampal damage leads to high circulating corticosterone levels.

Methods: The effects of mifepristone were investigated in 3xTg-AD mice using a combination of biochemical, histological, and behavior analyses.

Results: Mifepristone treatment rescues the pathologically induced cognitive impairments and markedly reduces amyloid beta (Aβ)-load and levels, as well as tau pathologies. Analysis of amyloid precursor protein (APP) processing revealed concomitant decreases in both APP C-terminal fragments C99 and C83 and the appearance of a larger 17-kDa C-terminal fragment. Hence, mifepristone induces a novel C-terminal cleavage of APP that prevents it being cleaved by α- or β-secretase, thereby precluding Aβ generation in the central nervous system; this cleavage and the production of the 17-kDa APP fragment was generated by a calcium-dependent cysteine protease. In addition, mifepristone treatment also reduced the phosphorylation and accumulation of tau, concomitant with reductions in p25. Notably, deficits in cyclic-AMP response element-binding protein signaling were restored with the treatment.

Conclusions: These preclinical results point to a potential therapeutic role for mifepristone as an effective treatment for AD and further highlight the impact the glucocorticoid system has as a regulator of Aβ generation.

Key Words: Amyloid beta, Alzheimer's disease, glucocorticoids, mifepristone, tau, 3xTg-AD

Alzheimer's disease (AD) is the most prevalent cause of dementia in the elderly, with only palliative treatments available at this time. It has been shown that AD patients display significant elevated levels of the glucocorticoid hormone cortisol in plasma and cerebrospinal fluid, as well as hypothalamic-pituitary-adrenal (HPA) axis dysfunction (1–3).

We previously showed that glucocorticoids (GCs) (cortisol in humans and corticosterone in rodents) could drive the formation of AD hallmark pathologies through increased production of the amyloid beta (Aβ) peptide and accumulation of somatodendritic tau (4). In addition, both stress and increased GC exposure have shown to induce cognitive impairments, trigger amyloid precursor protein (APP) misprocessing, reduce Aβ clearance by decreasing activity of insulin degrading enzyme (IDE), and stimulating tau hyperphosphorylation (5–9), together demonstrating a key role for GCs in the progression of AD pathology and cognitive decline. Glucocorticoids are key stress hormones secreted by the adrenal gland and controlled by the HPA axis, which mediate their effects in the different brain areas through two types of receptors: mineralocorticoid type I receptors and glucocorticoid type II receptors (GR) (10). Recently, the GR have been implicated in epigenetic mechanisms of neurodegeneration via histone deacetylase 2 (11).

The current study investigates the therapeutic potential of the glucocorticoid receptor antagonist mifepristone (RU486) on both cognitive and pathological outcomes in the 3xTg-AD mouse model of AD. 3xTg-AD mice show increased circulating levels of GCs from 9 months of age, when hippocampal pathology is advanced (4). Hence, we sought to evaluate if blocking the effects of GCs could help reduce pathology and cognitive decline in animals of this age. Here, we report that the GR blocker, mifepristone, has unparalleled effects on both outcomes, leading to robust reductions in Aβ levels and plaques through the induction of a 17-kDa cleavage of APP, precluding Aβ generation. In addition, it restores cyclic-AMP response element-binding protein (CREB) signaling and reduces tau hyperphosphorylation via reductions in p25 levels. Hence, our results show that compounds targeting the glucocorticoid system could be useful for the treatment of AD, in part through novel disease-modifying effects on Aβ generation.

Methods and Materials

Transgenic Mice and Treatment

All animal procedures were performed in accordance with National Institutes of Health and University of California guidelines and Use Committee at the University of California, Irvine. The characterization of 3xTg-AD mice has been described previously (12). In this study, 12-month-old homozygous non-transgenic (Ntg) and 3xTg-AD mice, 8 to 10 per group (male animals) were anesthetized with isoflurane and drug pellets containing the glucocorticoid receptor antagonist mifepristone (17b-hydroxy-11a-(4-dimethylaminophenyl)-17a-(1-propynyl)-

From the Department of Neurobiology and Behavior and Institute for Memory Impairments and Neurological Disorders, University of California, Irvine, Irvine, California.

Address correspondence to Kim N. Green, Ph.D., University of California, Irvine, Department of Neurobiology and Behavior, Institute for Memory Impairments and Neurological Disorders, 3208 Biological Sciences 3, Irvine, CA 92697-4545; E-mail: kngreen@uci.edu.

Received Aug 1, 2012; revised Dec 3, 2012; accepted Dec 6, 2012.

0006-3223/$36.00
http://dx.doi.org/10.1016/j.biopsych.2012.12.003

estra-4,9-dien-3-one) (Innovative Research of America, Sarasota, Florida) or vehicle pellets were implanted subcutaneous according to the manufacturer's instructions. In addition, 10-month-old homozygous 3xTg-AD mice, 10 per group (male animals) were anesthetized with isoflurane and drug pellets containing the selective glucocorticoid antagonist Cort-108297 ((R)-4a-Ethoxymethyl-1-(4-fluorophenyl)-6-(4-trifluoromethyl-benzenesulfonyl0-4,4a,5,6,7,8-hexahydro-1H-1,2,6-triaza-cyclopenta[b]naphthalene) (Corcept Therapeutics, Menlo Park, California) or vehicle pellets were implanted subcutaneous. The animals were treated for 21 days with 25.2 mg pellets that released a continuous flow of the drug at 1.2 mg per day (13–15).

Behavior Testing

Novel context, place, and object were conducted as described previously (16). Open field was performed as previously described (16). Hidden Morris water maze (MWM) tests were conducted as described previously (17,18). The passive inhibitory avoidance task was performed as described previously (19,20).

Tissue Preparation

Tissue preparation was performed as previously described (17,18). For protease analyses, whole brains were homogenized with/without complete protease inhibitor cocktail tablets (Roche Diagnostics GmbH, Mannheim, Germany) or specific families of protease inhibitor (leupeptin: 10 mg/mL; E64: 10 μmol/L; aprotinin: 10 mg/mL; pepstatin: 1 μmol/L; phosphoramidon: 10 μmol/L [Sigma–Aldrich, St. Louis, Missouri]), in the presence or absence of calcium in assay buffer (assay buffer: 135 mmol/L sodium chloride, 5 mmol/L potassium chloride, 1.2 mmol/L magnesium sulfate, 5 mmol/L N-2-hydroxyethylpiperazine-N′-2-ethanesulfonic acid, 10 mmol/L glucose, and 2.5 mmol/L calcium chloride). The samples were incubated 20 minutes at 37°C with the differences protease inhibitors and then immunoblotted for APP fragments using C-terminal antibody CT20 (Calbiochem, San Diego, California).

Immunohistochemistry

Immunohistochemistry for light microscopy was performed as we described previously (21). The following antibodies were used: anti-6E10 (1:1000; Covance Research Products, Denver, Pennsylvania) and PHF1 (1:1000; Pierce Biotechnology). The specificity of the immune reactions was controlled by omitting the primary antibody.

Total Aβ Loading

Quantification of total Aβ content was performed as previously described (21).

Immunoblotting

Immunoblot analyses were performed as described (4). The following primary antibodies were used: anti-CREB (1:1000; Cell Signaling), anti-phospho-CREB (ser133) (1:1000; Cell Signaling), anti-CTF20 (1:5000; Calbiochem) for C99 and C83, anti-HT7 (1:5000; Pierce Biotechnology), anti-AT8 (1:1000; Pierce Biotechnology), anti-AT180 (1:1000; Pierce Biotechnology), anti-AT270 (1:1000; Pierce Biotechnology), anti-PHF1 (Dr. Peter Davies, Albert Einstein College of Medicine, Manhasset, New York), anti-ADAM10 (1:1000; Calbiochem), anti-BACE (1:1000; Calbiochem), anti-IDE (1:1000; Chemicon), anti-total glycogen synthase kinase 3 (GSK3) α and β (1:5000; Calbiochem), anti-pGSK3β (ser9) (1:3000; Cell Signaling), anti-cyclin-dependent kinase 5 (Cdk5) (1:1000; Calbiochem), anti-C′-term p35 (1:200; Santa Cruz Biotechnology, Santa Cruz, California) for p25 and p35, anti-PP2A (1:1000; Santa Cruz Biotechnology), and anti-glyceraldehyde 3-phosphate dehydrogenase (1:5000; Santa Cruz Biotechnology).

Enzyme-Linked Immunosorbent Assay for $A\beta_{40}$ and $A\beta_{42}$

$A\beta_{1-40}$ and $A\beta_{1-42}$ were measured using a sensitive sandwich enzyme-linked immunosorbent assay system as previously described (4).

Mass Spectrometry of Mifepristone

Plasma (30 uL) was vortexed with 200 uL of dichloromethane, and the dichloromethane fraction was taken and air-dried. The precipitate was dissolved in 50 uL of 50% acetonitrile and then separated on an Acquity UltraPerformance LC (Waters Corporation, Milford, Massachusetts) and then analyzed on a Quatro Premier XE. Mifepristone standards showed fragments of molecular weight 134 and 370, which were positively identified in the plasma samples.

Quantitative and Statistical Analyses

All immunoblot data were quantitatively analyzed using ImageJ 1.4 software (Center for Information Technology National Institutes of Health, Bethesda, Maryland). Statistical evaluation of the results was performed using Student *t* test comparison to compare two groups or two-way analysis of variance (ANOVA). After significant analyses of variance, multiple post hoc comparisons were performed using Bonferroni's test. Analysis of MWM acquisition was evaluated via repeated measure of variance. The significance was set at 95% of confidence. All values are presented as mean ± SEM. All tests were performed using Graphpad Prism software (Graphpad Prism Inc., San Diego, California).

Results

Mifepristone Rescues Cognitive Deficits in Aged 3xTg-AD Mice

Male 3xTg-AD mice (12-month-old) were implanted with subcutaneous pellets containing 15 mg mifepristone or vehicle pellets designed to release a continuous flow of 10 μg per hour for 60 days. This concentration of mifepristone has proven effective to inhibit GR activity in mice (22,23). To determine whether mifepristone treatment could rescue cognitive deficits, 3xTg-AD mice were tested on a battery of behavioral tasks. Testing occurred during the last 2 weeks of treatment and probed cortical, hippocampal, and amygdala-dependent memory tasks, brain areas that are most severely affected by AD-like pathology in the 3xTg-AD (12,24).

Treated and vehicle-treated 3xTg-AD and Ntg mice were first tested on novel context/place/object tasks. These tasks are mainly hippocampal and cortical dependent, respectively. Vehicle-treated 3xTg-AD mice were significantly impaired compared with Ntg mice only on the novel object task, spending 50.17 ± 12.99% of their time exploring the out-of-context object, 47.09 ± 7.56% of their time exploring the out-of-place object, and 44.53 ± 9.87% of their time exploring the new object (Figure 1A–C), compared with Ntg mice. In contrast, mifepristone-treated 3xTg-AD mice showed a significant improvement in performance, spending 71.08 ± 11.30% of their time exploring the new object and 70.92 ± 7.70% of their time exploring the out-of-context object (Figure 1A,C). No differences

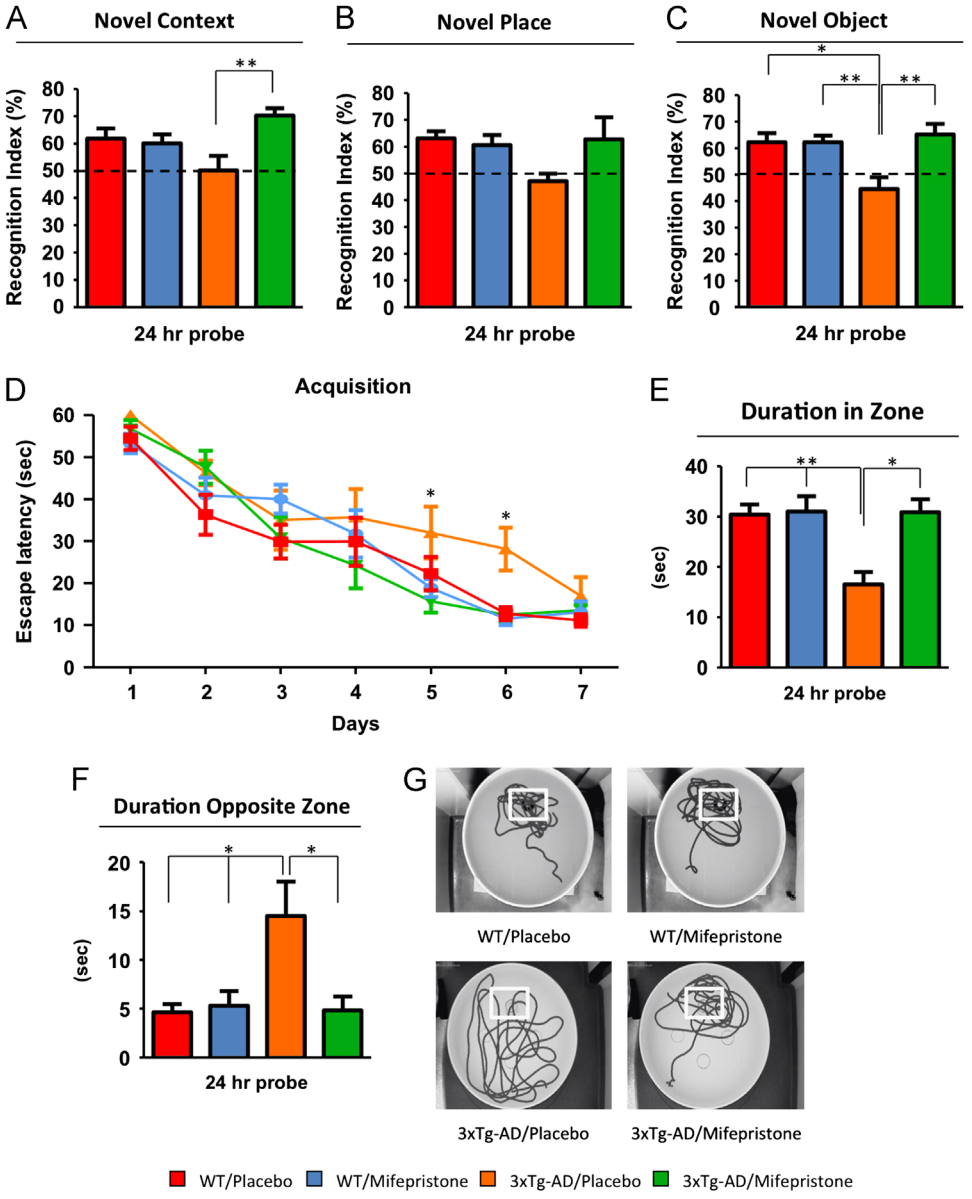

Figure 1. Mifepristone rescues cognitive impairments in 3xTg-AD mice. **(A–C)** Significant improvements in memory by novel context **(A)** and object **(C)** recognition were observed between mifepristone- and vehicle-treated 3xTg-AD mice. **(B)** No significant differences were detected in novel place. **(D)** Mice were trained on the spatial reference version of the Morris water maze (n = 8–10 per group). Acquisition curves shown for the 7 days of training on the Morris water maze. Mifepristone treatment reduces spatial memory deficits during training. **(E, F)** Mifepristone-treated mice shown significant improvements in duration spent in the target zone **(E)** and opposite zone **(F).** **(G)** Representative path tracings of the probe test session (white boxes represent localization of platform target). Nontransgenic-vehicle (red); Nontransgenic-mifepristone (blue); 3xTg-AD-vehicle (orange); 3xTg-AD-mifepristone (green). The values represent the mean ± SEM (n = 8–10). *$p < .05$ and **$p < .01$. WT, wild-type.

were observed between Ntg mifepristone and vehicle-treated mice (Figure 1A–C).

3xTg-AD mice were tested on another hippocampal-dependent behavior task, the MWM. Vehicle-treated 3xTg-AD mice reached criterion after 7 days (escape latency <25 seconds), whereas mifepristone-treated 3xTg-AD and Ntg vehicle and mifepristone-treated mice required only 5 days (Figure 1D). Furthermore, mifepristone treatment improved long-term memory (24-hour probe) in the 3xTg-AD mice compared with vehicle-treated mice, as determined by the significant increase in the duration of time in the platform quadrant and reduced time in the opposite quadrant (Figure 1E,F). These data were confirmed by the analysis of the swim patterns in the test session (Figure 1G). Notably, the effects of mifepristone on water maze performance were not directly related to motor alterations, since no significant variations of the swimming speed or total distance traveled in the water maze were observed in mifepristone compared with vehicle-treated mice (Figure S1A,B in Supplement 1).

In addition, no differences between vehicle- and mifepristone-treated mice were seen on the open field test (Figure S1C in Supplement 1). Finally, 3xTg-AD mice were trained in a contextual learning and memory task (passive inhibitory avoidance) primarily dependent on the amygdala (25). A 24-hour memory test revealed no differences between vehicle- and mifepristone-treated mice (Figure S1D in Supplement 1), pointing to a lack of improvement with mifepristone treatment. We confirmed the presence of mifepristone in the plasma at the end of the experiment via mass spectrometry.

Mifepristone Regulates CREB Signaling in 3xTg-AD but not Wild-Type Mice

Deficits in CREB signaling have been associated with impaired learning in 3xTg-AD mice (26). Western blot analyses of brain homogenates showed upregulation in steady-state levels of both CREB (41.17 ± 16.15%, two-way ANOVA, Bonferroni post hoc p = .07) and phospho-CREB (47.65 ± 9.20%, two-way ANOVA, Bonferroni post hoc p = .07) with mifepristone

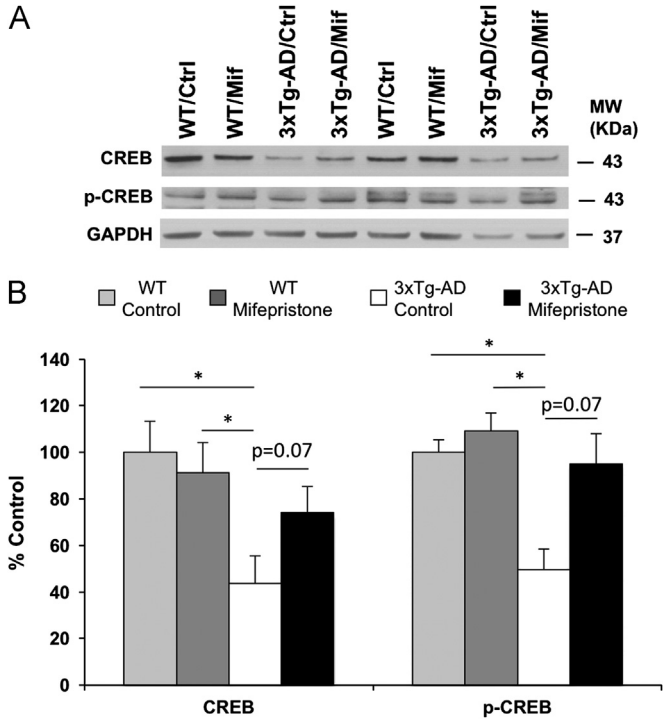

Figure 2. Mifepristone regulates cyclic-AMP response element-binding protein (CREB) signaling in 3xTg-AD. **(A)** Immunoblot analysis of CREB and phospho-CREB (p-CREB) from whole-brain homogenates of nontransgenic (Ntg) and 3xTg-AD mice treated for 2 months with either mifepristone (Mif) ($n = 8$) or vehicle (Ctrl) ($n = 8$) shown as alternating lanes. **(B)** Quantification of **(A)** normalized to glyceraldehyde 3-phosphate dehydrogenase (GAPDH) and expressed as a % of control shows significant increases in the steady-state level of CREB (41.17 ± 16.15%, two-way analysis of variance [ANOVA], Bonferroni post hoc, $p = .07$) and p-CREB (47.65 ± 9.20%, two-way ANOVA, Bonferroni post hoc, $p = .07$) in 3xTg-AD mice treated with mifepristone compared with vehicle. Notably, the quantifications show significant increases in steady-state level of CREB (56.40 ± 11.97%, two-way ANOVA, Bonferroni post hoc, $*p < .05$) and p-CREB (50.28 ± 8.74%, two-way ANOVA, Bonferroni post hoc, $*p < .05$) in Ntg compared with 3xTg-AD mice. Additionally, no differences in the steady-state level CREB and p-CREB in mifepristone-Ntg treated mice compared with vehicle. The values represent the mean ± SEM. $*p < .05$. MW, molecular weight; WT, wild-type.

treatment compared with vehicle. In addition, no differences were observed in Ntg mice in CREB or phospho-CREB with either vehicle or mifepristone. Notably, significant decreases (for CREB 56.40 ± 11.97%, two-way ANOVA, Bonferroni post hoc, $p < .05$, and for phospho-CREB 50.28 ± 8.74%, two-way ANOVA, Bonferroni post hoc, $p < .05$) in steady-state level of CREB and phospho-CREB were observed between Ntg and 3xTg-AD mice (Figure 2A,B).

Lower Aβ Levels and Plaque Load in Mifepristone-Treated 3xTg-AD Mice

Dramatic reductions in both soluble $A\beta_{40}$ (73.61 ± 10.56%, $p < .05$, *t* test) and $A\beta_{42}$ (74.06 ± 13.32%, $p < .05$, *t* test) were induced by mifepristone versus vehicle treatment (Figure 3A). In addition, insoluble $A\beta_{40}$ (72.12 ± 2.08%, $p < .05$, *t* test) and $A\beta_{42}$ (89.38 ± 7.92%, $p < .05$, *t* test) levels were robustly reduced in mifepristone treatment compared with vehicle mice (Figure 3B). In agreement with the enzyme-linked immunosorbent assay data, immunostaining analysis with antibody 6E10 showed intense reduction of extracellular deposits in mifepristone-treated compared with vehicle-treated mice (Figure 3C, 1–8); it should be noted that intracellular staining is likely due to a combination of Aβ as well as intracellular APP. Thus, the results showed a significant decrease in the subiculum (45.18 ± 10.16%, $p < .05$, *t* test) and cornu ammonis 1 hippocampal subfields (44.91 ± 7.70%, $p < .05$, *t* test) and the entorhinal cortex (64.91 ± 4.01%, $p < .05$, *t* test). Of significance to the cognitive data, we did not observe any significant changes in plaque load in the amygdala (Figure 3D). In addition, intracellular immunolabeling expression patterns were similar in mifepristone- and vehicle-treated mice in all analyzed brain areas (Figure 3C).

Mifepristone Induces a Novel 17-kDa APP Fragment that Precludes Aβ Generation

Steady-state levels of full-length APP holoprotein were unaffected by mifepristone treatment, as expected, as APP (and tau) were under the control of the thy1.2 transgene promoter in the 3xTg-AD mice. Using a C-terminal APP antibody [CT20 (27)], significant reductions in steady-state levels of both C83 (33.45 ± 7.49%, $p < .01$, *t* test) and C99 (36.88 ± 6.86%, $p < .05$, *t* test) were observed with mifepristone treatment (Figure 4A–C). Both C-terminal fragments (CTFs) were reduced by the same degree, which is unusual, as these fragments are usually mutually exclusive and also given no reductions in the parent holoprotein APP. Instead, we observed the appearance of a 17-kDa APP fragment only in mifepristone-treated animals; the 17-kDa fragment represented the last C′ 17-kDa of APP, which contained both the C99 and C83 sequence. As such, we deduced that this novel fragment was produced with mifepristone treatment and neither C99 nor C83 were produced, thus bypassing Aβ generation and explaining the concomitant reductions in both C99 and C83. We repeated this experiment using a different C-terminal antibody lot (Figure 4B), as a nonspecific band at 18-kDa was observed with the initial lot (Figure 4A). In confirmation of this pathway in the 3xTg-AD mice, we analyzed steady-state levels of endogenous APP and APP C-terminal fragments in Ntg mice treated with mifepristone. We found no changes in full length APP with mifepristone treatment but trended to reductions in the APP CTFs (27.32 ± 12.07%, $p = .08$, *t* test) compared with vehicle Ntg mice (Figure S2A,B in Supplement 1).

We analyzed steady-state levels of the constitutive protease α-secretase (ADAM10), β-secretase (BACE1) (28–31), and IDE (32), and found no differences with treatment (Figure 4D,E).

We reasoned that the protease responsible for the generation of the 17-kDa APP fragment was probably present in the brain but was unable to interact with APP under normal conditions. To test this, we took fresh brains from 3xTg-AD mice and homogenized them with our usual T-Per detergent buffer (Thermo Scientific, Rockford, Illinois) or a mild assay buffer with and without protease inhibitors. We found that brains homogenized in assay buffer in the absence of protease inhibitors generated the 17-kDa APP fragment (Figure 4F,H), but its production was blocked by the presence of protease inhibitors or by T-Per buffer. We then set to characterize the responsible APP protease further by incubating 3xTg-AD whole-brain homogenates in assay buffer for 20 minutes with specific proteases inhibitors. Brains incubated with leupeptin (serine and cysteine protease inhibitor) and E64 (cysteine protease inhibitor) blocked the formation of the 17-kDa C-terminal fragment. However, 3xTg-AD brain incubated with aprotinin (serine protease inhibitor), pepstatin (aspartyl protease inhibitor), and phosphoramidon (metalloendopeptidase inhibitor) was not able to block the formation of 17-kDa C-terminal fragment (Figure 4G,I). These data indicate that a cysteine

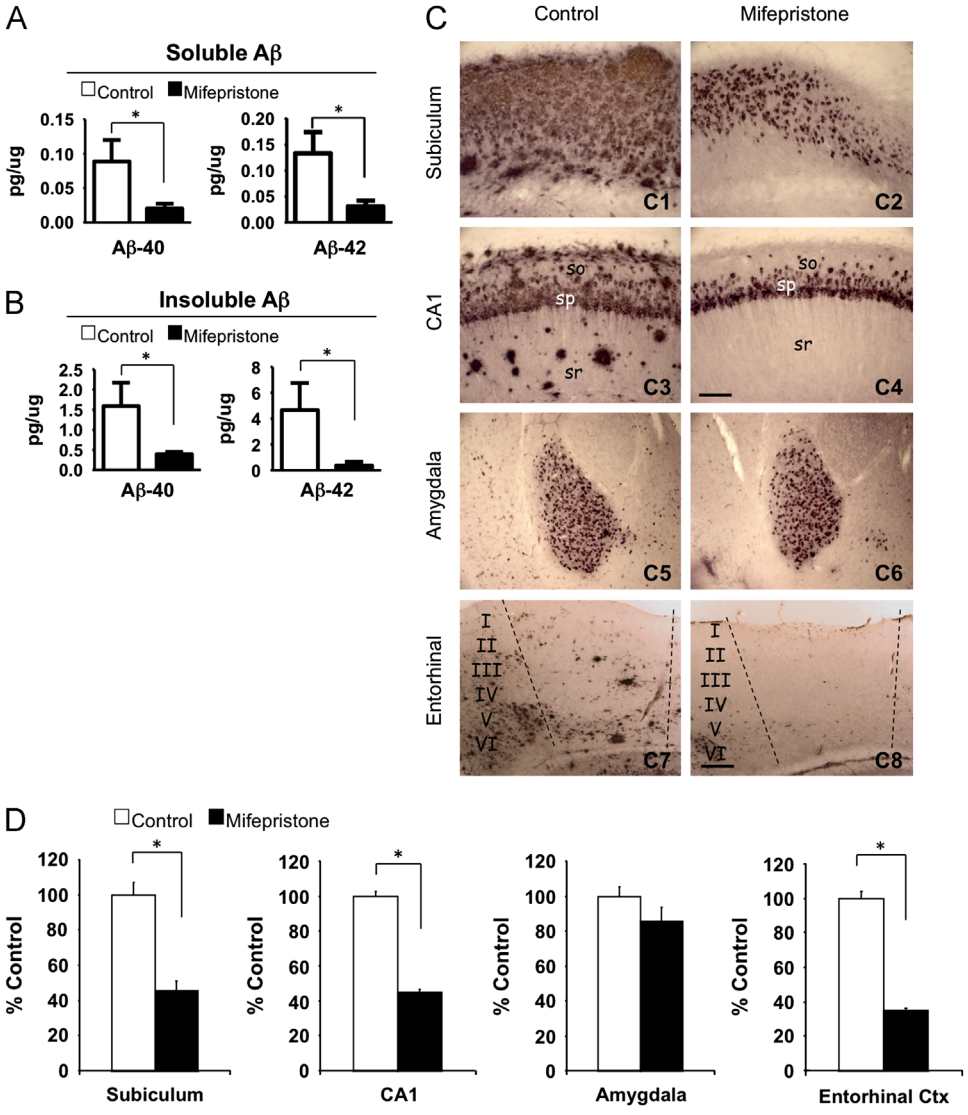

Figure 3. Mifepristone significantly lowers amyloid beta (Aβ) levels and plaque load. **(A, B)** Brain Aβ measurements by sandwich enzyme-linked immunosorbent assay of both the soluble ($A\beta_{40}$: 73.61 ± 10.56%, $^*p < .05$, *t* test; $A\beta_{42}$: 74.06 ± 13.32%, $^*p < .05$, *t* test) and insoluble ($A\beta_{40}$: 72.12 ± 2.08%, $^*p < .05$, *t* test; $A\beta_{42}$: 89.38 ± 7.92%, $^*p < .05$, *t* test) fractions of 3xTg-AD mice treated with mifepristone revealed dramatic reductions in Aβ levels. **(C)** Light microscopic images immunostained with anti-Aβ antibody (6E10) in the subiculum (C1 and C2), cornu ammonis 1 (CA1) (C3 and C4), amygdala (C5 and C6), and entorhinal cortex (C7 and C8) of 3xTg-AD in vehicle-treated (C1, 3, 5, and 7) and mifepristone-treated (C2, 4, 6, and 8) mice. **(D)** Quantitative plaque load analysis shows a significant decrease in hippocampal areas: subiculum (45.18 ± 10.16%, $^*p < .05$, *t* test) and CA1 (44.91 ± 7.70%, $^*p < .05$, *t* test); and entorhinal cortex (Ctx) (64.91 ± 4.01%, $^*p < .05$, *t* test). No significant differences were detected in the amygdala. Scale bars: 200 μm (C1–C4), 100 μm (C5–C8). The values represent the mean ± SEM. $^*p < .05$. so, stratum oriens; sp, stratum pyramidale; sr, stratum radiatum.

protease is involved in the formation of the 17-kDa C-terminal fragment in the 3xTg-AD mice. In addition, when brain samples were incubated in assay buffer without calcium and with ethylene glycol tetraacetic acid, the generation of the 17-kDa C-terminal fragment was blocked (Figure 4G, I). These data indicate that a calcium-dependent cysteine protease generates the 17-kDa C-terminal fragment in 3xTg-AD mice.

Mifepristone Reduces Accumulation of Tau Phosphorylated at Epitopes Thr181 and Ser396/404

Previous studies showed that glucocorticoids stimulate tau hyperphosphorylation and alter tau trafficking and stability (9,33). Subsequently, we examined the effects of mifepristone on tau phosphorylation. Western blot analyses of soluble brain homogenates revealed reductions in tau levels phosphorylated at residues Thr181 (46.89 ± 13.91%, $p < .05$, *t* test, and recognized by the AT270 antibody) and Ser396/404 (35.32 ± 13.69%, $p < .05$, *t* test, and recognized by the PHF1 antibody). Levels of phospho-tau species recognized by antibodies AT8 (Ser199/202) and AT180 (Thr231) were unaffected by mifepristone treatment versus vehicle treatment (Figure 5A,B). In correlation with biochemical analysis, immunohistochemistry of hippocampal sections (cornu ammonis 1 and subiculum) showed marked reductions in somatodendritic phospho-tau accumulation and aggregation in the pyramidal cell layer in the 3xTg-AD mifepristone-treated mice compared with vehicle (Figure 5C1–C4,C5). In addition, reductions in the number of dystrophic neurites positive for PHF1 were observed in the subiculum area of animals treated with mifepristone versus vehicle (Figure 5C6).

Finally, to elucidate the cellular mechanisms through which mifepristone reduces tau phosphorylation in the 3xTg-AD, we examined total and activated forms of Cdk5 and GSK3-β, two major kinases associated with abnormal tau phosphorylation in the brain (34–37). The results showed significant reductions in the steady-state levels of Cdk5 (32.66 ± 6.67%, $p < .05$, *t* test) and the cytosolic activator of Cdk5, p25 (35.32 ± 13.69%, $p < .05$, *t* test) in the mifepristone-treated mice (Figure 6D,E). Notably, we observed significant increases in steady-state levels of p35 (250.78 ± 8.34%, $p < .001$, *t* test) (Figure 5D,E). Similar results were observed in the steady-state levels of p25 in Ntg mice treated with mifepristone (46.64 ± 2.82%, $p < .01$, *t* test) (Figure S2C,D in Supplement 1) ; the cysteine protease calpain

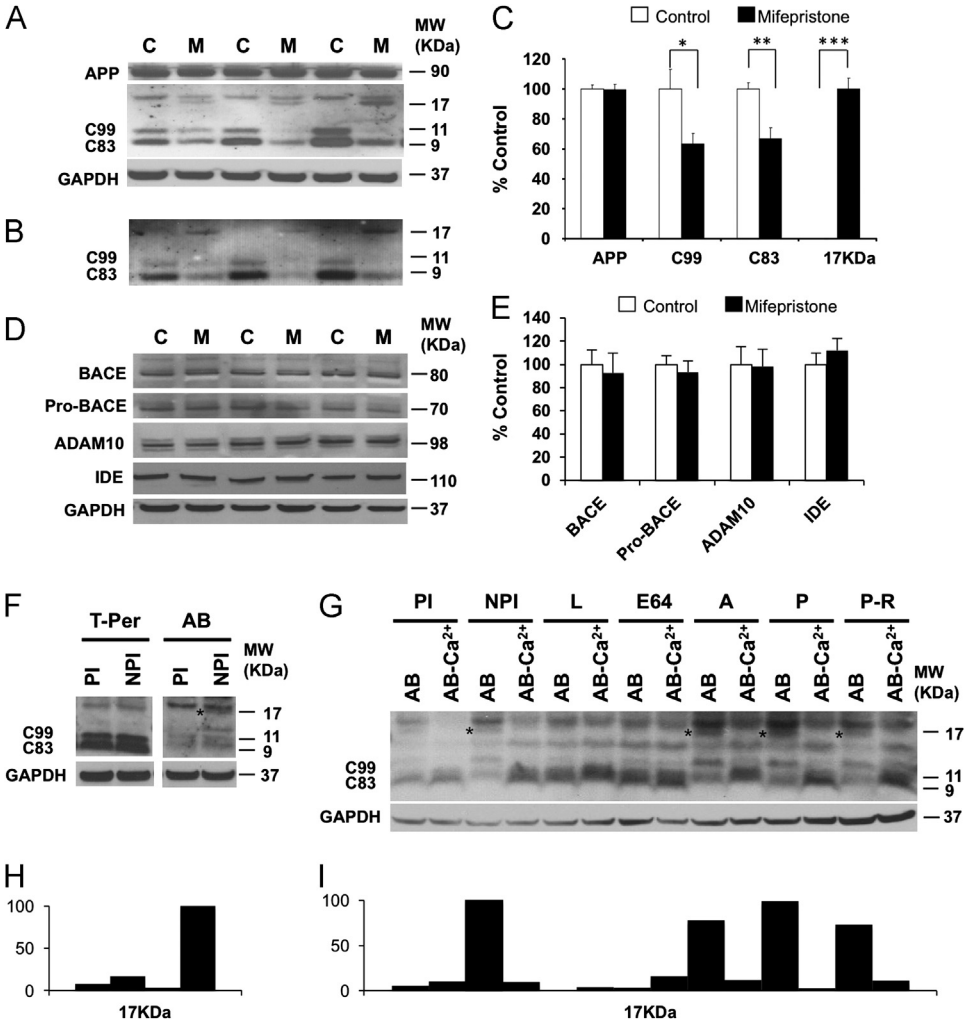

Figure 4. Mifepristone induces a novel 17-kDa amyloid precursor protein (APP) fragment and reduces both C99 and C83. **(A, B)** Immunoblot analysis of APP holoprotein, C99, C83, and a novel 17-kDa C-terminal APP fragment from whole-brain homogenates of 3xTg-AD mice treated for 2 months with either mifepristone (M) ($n = 8$) or vehicle (C) ($n = 8$) shown as alternating lanes. **(C)** Quantification of **(A)** and **(B)** normalized to glyceraldehyde 3-phosphate dehydrogenase (GAPDH) and expressed as a % of control shows a significant reduction of C99 (36.88 ± 6.86%, $^{*}p < .05$, *t* test) and C83 (33.45 ± 7.49%, $^{**}p < .01$, *t* test) in mifepristone-treated mice compared with vehicle. The appearance of the novel 17-kDa APP fragment was only seen with treatment ($^{***}p < .001$, *t* test). **(D)** Immunoblot analysis of BACE1, pro-BACE1, ADAM10, and insulin-degrading enzyme (IDE) from whole-brain homogenates of 3xTg-AD mice treated for 2 months with either mifepristone (M) ($n = 8$) or vehicle (C) ($n = 8$) shown as alternating lanes. **(E)** Quantification of **(D)** normalized to GAPDH and expressed as a % of control showed no significant differences in mifepristone-treated mice compare with vehicle. **(F)** and **(H)** Whole-brain homogenates were incubated using T-Per buffer and assay buffer (AB) with and without protease cocktail inhibitor and immunoblotted with a C-terminal APP antibody. *Denotes presence of 17-kDa APP fragment. **(G)** and **(I)** Whole-brain homogenates were incubated during 20 minutes at 37°C using assay buffer with/without protease inhibitors and specific protease inhibitor families and immunoblotted with a C-terminal APP antibody. *Denotes presence of 17-kDa APP fragment. The values represent the mean ± SEM ($n = 8$). $^{*}p < .05$, $^{**}p < .01$, and $^{***}p < .001$. A, aprotinin; AB-Ca^{2+}, assay buffer without Ca^{2+}; E64, trans-epoxysuccinyl-L-leucylamido-(4-guanidino)-butane; L, leupeptin; MW, molecular weight; NPI, nonprotease inhibitors; P, pepstatin; PI, protease inhibitors; P-R, phosphoramidon.

mediates the proteolytic cleavage of p35 to p25 (38), suggesting that mifepristone could inhibit calpain activity. Steady-state levels of GSK3-β, pS9-GSK3-β (inactive GSK3-β phosphorylated at ser9), extracellular signal-regulated kinase, phosphorylated extracellular signal-regulated kinase, c-Jun N-terminal kinase, phospho-c-Jun N-terminal kinase, and PP2A (tau phosphatase), were unaffected by mifepristone treatment (Figure 5D,E). In correlation with the cognitive data, immunostaining analysis of the amygdala showed no differences in the expression of total human tau, while similar low numbers of PHF1 positive cells were observed in both 3xTg-AD vehicle- and mifepristone-treated mice (Figure S3A,B in Supplement 1). Our results indicate that mifepristone mediates reduction of phospho-tau levels on residues Thr181 and Ser396/404 correlating with inactivation of Cdk5/p25 in the 3xTg-AD.

A Specific GR Antagonist Reduces APP CTFs and p25

Mifepristone is an antagonist at both the GR and progesterone receptor (PR). To explore which of these targets were mediating the effects seen in the 3xTg-AD mice, we obtained the specific GR antagonist Cort-108297 (13–15) (a generous gift from Corcept Therapeutics). We manufactured slow-release pellets and implanted them, or placebo pellets, subcutaneous for 21 days. At the end of this period, we analyzed brain homogenates for APP fragments, Aβ and p25 levels (Figure 6A–F). Consistent with mifepristone treatment, Cort-108297 significantly reduced levels of C83 (35.32 ± 8.02%, $p < .05$, *t* test) and trended toward a decrease in C99. Likewise, levels of p25 (48.02 ± 34.19%, $p < .05$, *t* test) were significantly reduced with treatment. However, levels of Aβ were not significantly reduced, but this could be related to the shorter treatment duration than the experiments performed with mifepristone.

Discussion

There is ample evidence implicating HPA axis dysfunction in AD, reflected by markedly elevated basal levels of circulating cortisol and a failure to show cortisol suppression following a dexamethasone challenge (1–3). We previously demonstrated that elevated circulating glucocorticoids could rapidly increase levels of both Aβ and tau protein in the brains of transgenic mice (4), whereas others showed similar results through changes in Aβ

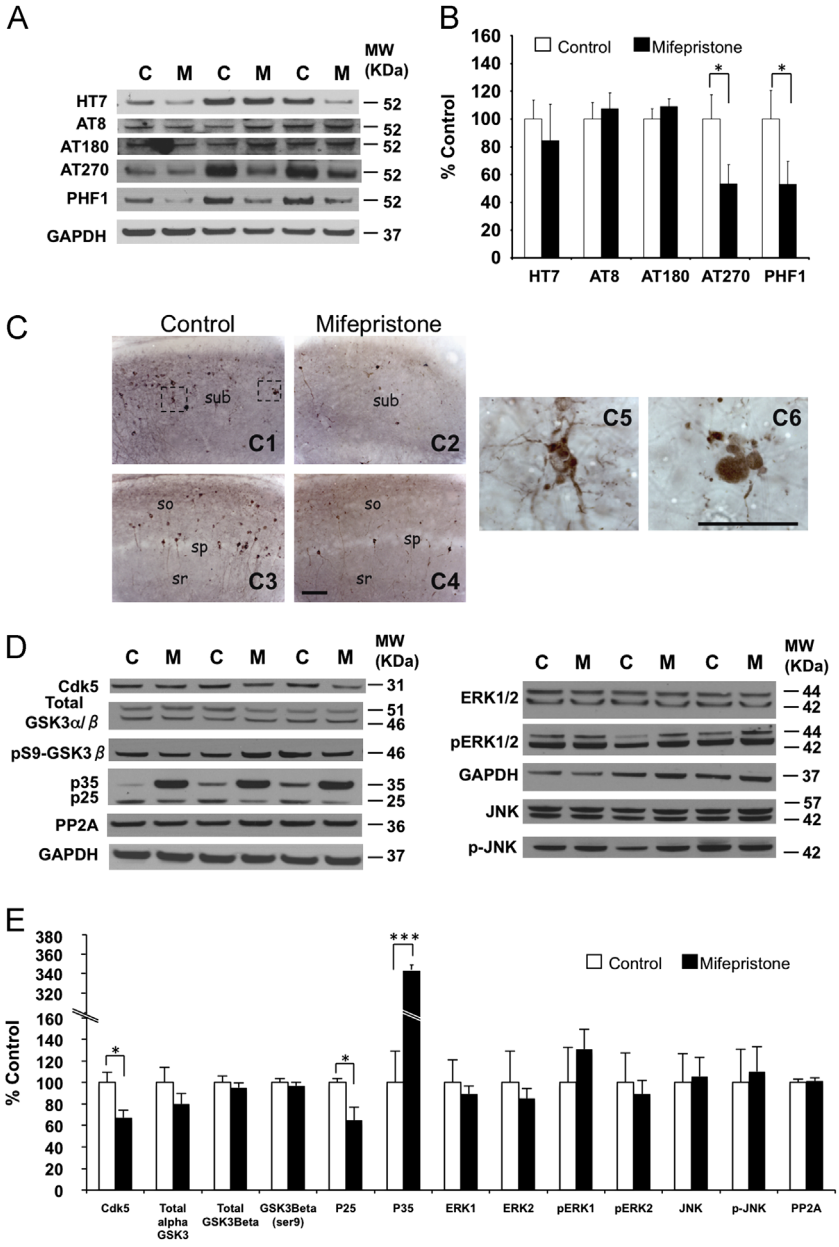

Figure 5. Mifepristone reduces accumulation of p-tau epitopes Thr181 and Ser396/404. **(A)** Immunoblot analysis of total tau (HT7) and phospho-tau epitopes including pSer199/202 tau (AT8), pThr231 (AT180), pThr181 (AT270), and pSer396/404 (PHF1) of protein extracts from whole-brain homogenates of 3xTg-AD mice treated for 2 months with either mifepristone (M) ($n = 8$) or vehicle (C) ($n = 8$) shown as alternating lanes. **(B)** Quantification of **(A)** normalized to glyceraldehyde 3-phosphate dehydrogenase (GAPDH) and expressed as a % of control shows significant reductions in p-tau epitopes Thr181 (46.89 ± 13.91%, $^*p < .05$, *t* test) and Ser 396/404 (47.20 ± 16.88%, $^*p < .05$, *t* test). **(C)** Light microscopic images immunostained with anti-pSer396/404 antibody (PHF1 antibody) in the hippocampus (subiculum: C1 and C2; cornu ammonis 1: C3 and C4) of 3xTg-AD in control (C1 and C3) and mifepristone-treated (C2 and C4) mice at 14 months of age. Intracellular p-tau (pSer396/404) accumulation and aggregation (C1) and a dystrophy neurite positive for pSer396/404 are shown in enlarged images. **(D)** Immunoblot analysis of cyclin-dependent kinase 5 (Cdk5), glycogen synthase kinase 3 (GSK3) α/β, inactive GSK3β (phosphorylated at ser9), p25/p35, PP2A, extracellular signal-regulated kinase (ERK), phosphorylated extracellular signal-regulated kinase (pERK), c-Jun N-terminal kinase (JNK) and phospho-c-Jun N-terminal kinase (p-JNK) of protein extracts from whole-brain homogenates of 3xTg-AD mice treated for 2 months with either mifepristone (M) ($n = 8$) or vehicle (C) ($n = 8$) shown as alternating lanes. **(E)** Quantification of **(D)** normalized to GAPDH and expressed as a % of control shows significant reductions in the expression of Cdk5 (32.66 ± 6.67%, $^*p < .05$, *t* test) and p25 (35.32 ± 13.69%, $^*p < .05$, *t* test). Furthermore, accumulation of p35 (250.78 ± 8.34%, $^{***}p < .001$, *t* test) was observed in 3xTg-AD mifepristone-treated mice. Scale bars: 200 μm (C1–C4), 50 μm (C5 and C6). Glyceraldehyde 3-phosphate dehydrogenase levels were used as control for protein loading. The values represent the mean ± SEM. $^*p < .05$ and $^{***}p < .001$. MW, molecular weight; so, stratum oriens; sp, stratum pyramidale; sr, stratum radiatum; sub, subiculum.

degradation and increases in tau phosphorylation, suggesting that these elevated cortisol levels in AD could drive some of the pathological progression (5–9). Recently, the corticotropin-releasing factor receptor has also been implicated in the progression of tau pathology, highlighting a link between stress and AD (39). In addition, it is known that prolonged exposure and high levels of GCs is associated with neuronal damage and cognitive decline in the central nervous system (CNS) (40–42). Thus, we investigated if antiglucocorticoid strategies could offer a viable therapeutic approach.

This study shows clear cognitive improvements in a number of domains with treatment of aged 3xTg-AD mice with the glucocorticoid and progesterone receptor blocker mifepristone. Although these improvements are likely due to the marked reductions in both Aβ and tau pathologies in mifepristone-treated mice, antiglucocorticoid drugs, through 11-β hydroxysteroid dehydrogenase inhibitors, have recently been shown to improve cognition in aged mice of their own (43,44). Of note, a small clinical trial in AD patients treated with mifepristone for just 6 weeks reported an increase in the Alzheimer's Disease Assessment Scale-Cognitive Subscale (45), although this short time frame is unlikely to have reversed pathology in humans.

Although glucocorticoid-reducing compounds may exhibit cognitive-enhancing capabilities on their own, treatment with mifepristone led to profound reductions in both soluble and insoluble Aβ levels in the 3xTg-AD mice. These reductions in Aβ appear to be due to the induction of a novel APP processing pathway in which APP is cleaved 17-kDa from the C-terminal, by an unidentified protease, rather than by either α-secretase or β-secretase. As such, C99 (and C83) formation is prevented, and by extension, so is Aβ formation. We recently described this novel APP processing pathway in the CNS of AD transgenic mice and cynomolgus primates using a small molecular compound known as ST101, with no known molecular

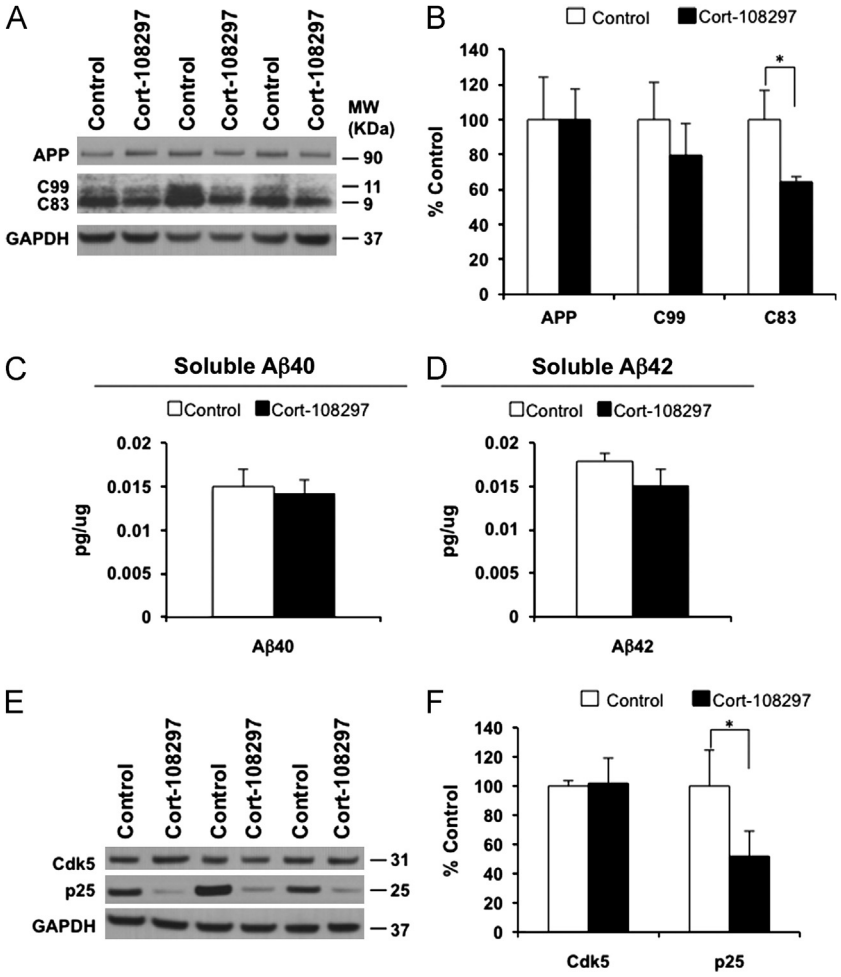

Figure 6. The selective Cort-108297 glucocorticoid antagonist reduces C-terminal amyloid beta precursor protein (APP) fragment and p25 expression. **(A)** Immunoblot analysis of APP holoprotein, C99, and C83 C-terminal APP fragment from whole-brain homogenates of 3xTg-AD mice treated for 21 days with either Cort-108297 (Cort-108297) ($n = 8$) or vehicle (Control) ($n = 8$) shown as alternating lanes. **(B)** Quantification of **(A)** normalized to glyceraldehyde 3-phosphate dehydrogenase (GAPDH) and expressed as a % of control shows a significant reduction of C83 (35.32 ± 8.02%, $^*p < .05$, *t* test) in Cort-108297-treated mice compared with vehicle. In addition, a decreased tendency in steady-state levels was observed with C99. **(C)** and **(D)** Brain amyloid beta (Aβ) measurements by sandwich enzyme-linked immunosorbent assay of both soluble $A\beta_{40}$ and $A\beta_{42}$ of 3xTg-AD mice treated with Cort-108297. **(E)** Immunoblot analysis of cyclin-dependent kinase 5 (Cdk5) and p25 of protein extracts from whole-brain homogenates of 3xTg-AD mice treated for 21 days with Cort-108297 (Cort-108297) ($n = 8$) or vehicle (Control) ($n = 8$) shown as alternating lanes. **(F)** Quantification of **(E)** normalized to GAPDH and expressed as a % of control shows significant reductions in the expression of p25 (48.02 ± 34.19%, $^*p < .05$, *t* test). Glyceraldehyde 3-phosphate dehydrogenase levels were used as control for protein loading. The values represent the mean ± SEM. $^*p < .05$.

targets or mechanisms of action (46). Here, we show that mifepristone stimulates the same novel APP processing pathway and leads to larger reductions in AD-related pathology, as well as robust improvements in cognition. We hypothesize that mifepristone is either modulating the activity of this unknown APP protease or that it is altering the subcellular location of either APP or the protease such that they can interact in the presence of mifepristone. To this end, we show that the untreated brain has the ability to make this 17-kDa APP fragment in the absence of protease inhibitors, showing that the protease is always present but does not normally cleave APP. Furthermore, we find that only inhibitors of cysteine proteases can block the formation of this APP fragment, and that calcium is necessary. Thus, an APP calcium-dependent cysteine protease exists but its identity is unknown. Prominent calcium-dependent cysteine proteases include the calpains—here, we find that mifepristone down-regulates p25 levels, which themselves are a product of calpain activity. Thus, it is unlikely that calpains are the unidentified APP protease, and further experiments will be required to fully identify it. Mifepristone also attenuated tau pathology in the 3xTg-AD mice, through reduction of steady-state levels of phospho-tau on residues Thr181 and Ser396/404, concomitant with reductions in p25 in both Ntg and 3xTg-AD mice. We also observed significant reductions in the number of cell and dystrophic neurites positive for PHF1 in 3xTg-AD treated with mifepristone versus vehicle. In agreement with this, previous studies have shown that elevated GCs can increase tau phosphorylation (9,33).

In addition, the PR has been implicated in both cognitive improvements (47,48) and reductions in pathology (49,50) in mouse models of AD. For example, the progesterone metabolite allopregnanolone improves cognition in the 3xTg-AD mice via increases in neurogenesis (51,52) and reduces Aβ accumulation (53), and progesterone itself improves cognition in APP mice (49) and also reduces tau hyperphosphorylation in 3xTg-AD mice (50). Notably, mifepristone can be metabolized in both the periphery and CNS (54), and these newly formed metabolites can bind to both the GR and PR (55). Furthermore, treatment with a specific GR antagonist, Cort-108297, was able to reduce APP CTFs and p25, thus mimicking some of the effects of mifepristone. These results suggest that the effect observed by mifepristone is related by modulation of GC instead of PR receptor. However, we cannot discard that PR or other steroid receptor could be modulated by mifepristone. Future research using knockout mice for GR, PR, or other steroid hormone will be necessary to elucidate the effect of mifepristone to these receptors.

Cyclic-AMP response element-binding protein signaling is impaired in 3xTg-AD mice, and restoration of CREB signaling restores cognitive function (26). Hence, we next looked at levels of CREB and phospho-CREB and found both to be significantly increased in mifepristone-treated mice versus vehicle. Notably, no effects were seen in Ntg mice. These results suggest that 1) the

effects on CREB signaling are mediated by the reductions in pathology rather than a direct effect of mifepristone, as the wild-type mice were not affected; and 2) increases in CREB signaling could be mediating the improved cognition in the 3xTg-AD mice.

Hence, mifepristone and other GR targeting strategies may offer potential benefit for the treatment of AD.

This work was supported, in part, by grants from the National Institutes of Health AG-021982 to FML. Amyloid beta peptides and anti-amyloid beta antibodies were provided by the University of California Alzheimer's Disease Research Center National Institutes of Health/National Institute on Aging Grant P50 AG16573.

We thank Corcept Therapeutics for the generous gift of Cort-108297.

All authors declare no biomedical financial interests or potential conflicts of interest.

Supplementary material cited in this article is available online.

1. Csernansky JG, Dong H, Fagan AM, Wang L, Xiong C, Holtzman DM, Morris JC (2006): Plasma cortisol and progression of dementia in subjects with Alzheimer-type dementia. *Am J Psychiatry* 163: 2164–2169.
2. Hoogendijk WJ, Meynen G, Endert E, Hofman MA, Swaab DF (2006): Increased cerebrospinal fluid cortisol level in Alzheimer's disease is not related to depression. *Neurobiol Aging* 27:780.e1–780.e2.
3. Umegaki H, Ikari H, Nakahata H, Endo H, Suzuki Y, Ogawa O, *et al.* (2000): Plasma cortisol levels in elderly female subjects with Alzheimer's disease: A cross-sectional and longitudinal study. *Brain Res* 881: 241–243.
4. Green KN, Billings LM, Roozendaal B, McGaugh JL, LaFerla FM (2006): Glucocorticoids increase amyloid-beta and tau pathology in a mouse model of Alzheimer's disease. *J Neurosci* 26:9047–9056.
5. Catania C, Sotiropoulos I, Silva R, Onofri C, Breen KC, Sousa N, Almeida OF (2009): The amyloidogenic potential and behavioral correlates of stress. *Mol Psychiatry* 14:95–105.
6. Jeong YH, Park CH, Yoo J, Shin KY, Ahn SM, Kim HS, *et al.* (2006): Chronic stress accelerates learning and memory impairments and increases amyloid deposition in APPV717I-CT100 transgenic mice, an Alzheimer's disease model. *FASEB J* 20:729–731.
7. Kulstad JJ, McMillan PJ, Leverenz JB, Cook DG, Green PS, Peskind ER, *et al.* (2005): Effects of chronic glucocorticoid administration on insulin-degrading enzyme and amyloid-beta peptide in the aged macaque. *J Neuropathol Exp Neurol* 64:139–146.
8. Lim GP, Yang F, Chu T, Chen P, Beech W, Teter B, *et al.* (2000): Ibuprofen suppresses plaque pathology and inflammation in a mouse model for Alzheimer's disease. *J Neurosci* 20:5709–5714.
9. Sotiropoulos I, Catania C, Riedemann T, Fry JP, Breen KC, Michaelidis TM, Almeida OF (2008): Glucocorticoids trigger Alzheimer disease-like pathobiochemistry in rat neuronal cells expressing human tau. *J Neurochem* 107:385–397.
10. Reul JM, de Kloet ER (1985): Two receptor systems for corticosterone in rat brain: Microdistribution and differential occupation. *Endocrinology* 117:2505–2511.
11. Graff J, Rei D, Guan JS, Wang WY, Seo J, Hennig KM, *et al.* (2012): An epigenetic blockade of cognitive functions in the neurodegenerating brain. *Nature* 483:222–226.
12. Oddo S, Caccamo A, Shepherd JD, Murphy MP, Golde TE, Kayed R, *et al.* (2003): Triple-transgenic model of Alzheimer's disease with plaques and tangles: Intracellular Abeta and synaptic dysfunction. *Neuron* 39:409–421.
13. Andrade C, Shaikh SA, Narayan L, Blasey C, Belanoff J (2012): Administration of a selective glucocorticoid antagonist attenuates electroconvulsive shock-induced retrograde amnesia. *J Neural Transm* 119:337–344.
14. Asagami T, Belanoff JK, Azuma J, Blasey CM, Clark RD, Tsao PS (2011): Selective glucocorticoid receptor (GR-II) antagonist reduces body weight gain in mice. *J Nutr Metab* 2011:235389.
15. Belanoff JK, Blasey CM, Clark RD, Roe RL (2010): Selective glucocorticoid receptor (type II) antagonist prevents and reverses olanzapine-induced weight gain. *Diabetes Obes Metab* 12:545–547.
16. Ennaceur A, Delacour J (1988): A new one-trial test for neurobiological studies of memory in rats. 1: Behavioral data. *Behav Brain Res* 31:47–59.
17. Billings LM, Oddo S, Green KN, McGaugh JL, LaFerla FM (2005): Intraneuronal Abeta causes the onset of early Alzheimer's disease-related cognitive deficits in transgenic mice. *Neuron* 45:675–688.
18. Medeiros R, Kitazawa M, Caccamo A, Baglietto-Vargas D, Estrada-Hernandez T, Cribbs DH, *et al.* (2011): Loss of muscarinic m(1) receptor exacerbates Alzheimer's disease-like pathology and cognitive decline. *Am J Pathol* 179:980–991.
19. Clinton LK, Billings LM, Green KN, Caccamo A, Ngo J, Oddo S, *et al.* (2007): Age-dependent sexual dimorphism in cognition and stress response in the 3xTg-AD mice. *Neurobiol Dis* 28:76–82.
20. Martinez-Coria H, Green KN, Billings LM, Kitazawa M, Albrecht M, Rammes G, *et al.* (2010): Memantine improves cognition and reduces Alzheimer's-like neuropathology in transgenic mice. *Am J Pathol* 176:870–880.
21. Baglietto-Vargas D, Moreno-Gonzalez I, Sanchez-Varo R, Jimenez S, Trujillo-Estrada L, Sanchez-Mejias E, *et al.* (2010): Calretinin interneurons are early targets of extracellular amyloid-beta pathology in PS1/AbetaPP Alzheimer mice hippocampus. *J Alzheimers Dis* 21:119–132.
22. Kruszewska B, Felten DL, Stevens SY, Moynihan JA (1998): Sympathectomy-induced immune changes are not abrogated by the glucocorticoid receptor blocker RU-486. *Brain Behav Immun* 12:181–200.
23. Pastva A, Estell K, Schoeb TR, Schwiebert LM (2005): RU486 blocks the anti-inflammatory effects of exercise in a murine model of allergen-induced pulmonary inflammation. *Brain Behav Immun* 19:413–422.
24. Oddo S, Caccamo A, Kitazawa M, Tseng BP, LaFerla FM (2003): Amyloid deposition precedes tangle formation in a triple transgenic model of Alzheimer's disease. *Neurobiol Aging* 24:1063–1070.
25. McGaugh JL, McIntyre CK, Power AE (2002): Amygdala modulation of memory consolidation: Interaction with other brain systems. *Neurobiol Learn Mem* 78:539–552.
26. Caccamo A, Maldonado MA, Bokov AF, Majumder S, Oddo S (2010): CBP gene transfer increases BDNF levels and ameliorates learning and memory deficits in a mouse model of Alzheimer's disease. *Proc Natl Acad Sci U S A* 107:22687–22692.
27. Pinnix I, Musunuru U, Tun H, Sridharan A, Golde T, Eckman C, *et al.* (2001): A novel gamma-secretase assay based on detection of the putative C-terminal fragment-gamma of amyloid beta protein precursor. *J Biol Chem* 276:481–487.
28. Allinson TM, Parkin ET, Turner AJ, Hooper NM (2003): ADAMs family members as amyloid precursor protein alpha-secretases. *J Neurosci Res* 74:342–352.
29. Lammich S, Kojro E, Postina R, Gilbert S, Pfeiffer R, Jasionowski M, *et al.* (1999): Constitutive and regulated alpha-secretase cleavage of Alzheimer's amyloid precursor protein by a disintegrin metalloprotease. *Proc Natl Acad Sci U S A* 96:3922–3927.
30. Postina R, Schroeder A, Dewachter I, Bohl J, Schmitt U, Kojro E, *et al.* (2004): A disintegrin-metalloproteinase prevents amyloid plaque formation and hippocampal defects in an Alzheimer disease mouse model. *J Clin Invest* 113:1456–1464.
31. Vassar R, Bennett BD, Babu-Khan S, Kahn S, Mendiaz EA, Denis P, *et al.* (1999): Beta-secretase cleavage of Alzheimer's amyloid precursor protein by the transmembrane aspartic protease BACE. *Science* 286:735–741.
32. Selkoe DJ (2001): Clearing the brain's amyloid cobwebs. *Neuron* 32: 177–180.
33. Rissman RA, Lee KF, Vale W, Sawchenko PE (2007): Corticotropin-releasing factor receptors differentially regulate stress-induced tau phosphorylation. *J Neurosci* 27:6552–6562.
34. Gong CX, Liu F, Grundke-Iqbal I, Iqbal K (2005): Post-translational modifications of tau protein in Alzheimer's disease. *J Neural Transm* 112:813–838.
35. Hanger DP, Hughes K, Woodgett JR, Brion JP, Anderton BH (1992): Glycogen synthase kinase-3 induces Alzheimer's disease-like phosphorylation of tau: Generation of paired helical filament epitopes and neuronal localisation of the kinase. *Neurosci Lett* 147:58–62.
36. Medeiros R, Baglietto-Vargas D, Laferla FM (2011): The role of tau in Alzheimer's disease and related disorders. *CNS Neurosci Ther* 17:514–524.
37. Noble W, Olm V, Takata K, Casey E, Mary O, Meyerson J, *et al.* (2003): Cdk5 is a key factor in tau aggregation and tangle formation in vivo. *Neuron* 38:555–565.

38. Lee MS, Kwon YT, Li M, Peng J, Friedlander RM, Tsai LH (2000): Neurotoxicity induces cleavage of p35 to p25 by calpain. *Nature* 405: 360–364.
39. Carroll JC, Iba M, Bangasser DA, Valentino RJ, James MJ, Brunden KR, *et al*. (2011): Chronic stress exacerbates tau pathology, neurodegeneration, and cognitive performance through a corticotropin-releasing factor receptor-dependent mechanism in a transgenic mouse model of tauopathy. *J Neurosci* 31:14436–14449.
40. Elgh E, Lindqvist Astot A, Fagerlund M, Eriksson S, Olsson T, Nasman B (2006): Cognitive dysfunction, hippocampal atrophy and glucocorticoid feedback in Alzheimer's disease. *Biol Psychiatry* 59:155–161.
41. McEwen BS (2001): Plasticity of the hippocampus: Adaptation to chronic stress and allostatic load. *Ann N Y Acad Sci* 933:265–277.
42. Nichols NR, Zieba M, Bye N (2001): Do glucocorticoids contribute to brain aging? *Brain Res Brain Res Rev* 37:273–286.
43. Sooy K, Webster SP, Noble J, Binnie M, Walker BR, Seckl JR, Yau JL (2010): Partial deficiency or short-term inhibition of 11beta-hydroxysteroid dehydrogenase type 1 improves cognitive function in aging mice. *J Neurosci* 30:13867–13872.
44. Mohler EG, Browman KE, Roderwald VA, Cronin EA, Markosyan S, Scott Bitner R, *et al*. (2011): Acute inhibition of 11beta-hydroxysteroid dehydrogenase type-1 improves memory in rodent models of cognition. *J Neurosci* 31:5406–5413.
45. Pomara N, Doraiswamy PM, Tun H, Ferris S (2002): Mifepristone (RU 486) for Alzheimer's disease. *Neurology* 58:1436.
46. Green KN, Khashwji H, Estrada T, Laferla FM (2011): ST101 induces a novel 17 kDa APP cleavage that precludes Abeta generation in vivo. *Ann Neurol* 69:831–844.
47. Gibson CL, Murphy SP (2004): Progesterone enhances functional recovery after middle cerebral artery occlusion in male mice. *J Cereb Blood Flow Metab* 24:805–813.
48. He J, Hoffman SW, Stein DG (2004): Allopregnanolone, a progesterone metabolite, enhances behavioral recovery and decreases neuronal loss after traumatic brain injury. *Restor Neurol Neurosci* 22:19–31.
49. Frye CA, Walf AA (2008): Effects of progesterone administration and APPswe+PSEN1Deltae9 mutation for cognitive performance of mid-aged mice. *Neurobiol Learn Mem* 89:17–26.
50. Carroll JC, Rosario ER, Chang L, Stanczyk FZ, Oddo S, LaFerla FM, Pike CJ (2007): Progesterone and estrogen regulate Alzheimer-like neuropathology in female 3xTg-AD mice. *J Neurosci* 27:13357–13365.
51. Singh C, Liu L, Wang JM, Irwin RW, Yao J, Chen S, *et al*. (2012): Allopregnanolone restores hippocampal-dependent learning and memory and neural progenitor survival in aging 3xTgAD and nonTg mice. *Neurobiol Aging* 33:1493–1506.
52. Wang JM, Singh C, Liu L, Irwin RW, Chen S, Chung EJ, *et al*. (2010): Allopregnanolone reverses neurogenic and cognitive deficits in mouse model of Alzheimer's disease. *Proc Natl Acad Sci U S A* 107:6498–6503.
53. Chen S, Wang JM, Irwin RW, Yao J, Liu L, Brinton RD (2011): Allopregnanolone promotes regeneration and reduces beta-amyloid burden in a preclinical model of Alzheimer's disease. *PloS One* 6:e24293.
54. Lin HL, Zhang H, Hollenberg PF (2009): Metabolic activation of mifepristone [RU486; 17beta-hydroxy-11beta-(4-dimethylaminophenyl)-17alpha-(1-propynyl)-estra-4,9-dien -3-one] by mammalian cytochromes P450 and the mechanism-based inactivation of human CYP2B6. *J Pharmacol Exp Ther* 329:26–37.
55. Heikinheimo O, Kontula K, Croxatto H, Spitz I, Luukkainen T, Lahteenmaki P (1987): Plasma concentrations and receptor binding of RU 486 and its metabolites in humans. *J Steroid Biochem* 26: 279–284.